Computers and Concrete, *Vol. 19, No. 3 (2017) 243-256*
DOI: https://doi.org/10.12989/cac.2017.19.3.243

Influence of different fatigue loads and coating thicknesses on service performance of RC beam specimens with epoxy-coated reinforcement

Xiao-Hui Wang[*1,2], Yang Gao[3], Run-Dong Gao[4], Jing Wang[2] and Xi-La Liu[2]

[1]*School of Energy, Geoscience, Infrastructure and Society, Heriot-Watt University, EH14 4AS, Edinburgh, UK*
[2]*Dept. of Civil Engineering, Shanghai Jiao Tong Univ., No. 800 Dongchuan Rd., 200240, Shanghai, P.R. China*
[3]*Shanghai Municipal Engineering Design Institute (Group) Co., LTD, 200092, Shanghai, P.R. China*
[4]*Shanghai Key Laboratory of Engineering Structure Safety, 200032, Shanghai, P.R. China*

(Received October 16, 2014, Revised November 12, 2016, Accepted December 22, 2016)

Abstract. Epoxy-coated reinforcing bars are widely used to protect the corrosion of the reinforcing bars in the RC elements under their in-service environments and external loads. In most field surveys, it was reported that the corrosion resistance of the epoxy-coated reinforcing bars is typically better than the uncoated bars. However, from the experimental tests conducted in the labs, it was reported that, under the same loads, the RC elements with epoxy-coated reinforcing bars had wider cracks than the elements reinforced with the ordinary bars. Although this conclusion may be true considering the bond reduction of the reinforcing bar due to the epoxy coating, the maximum service loads used in the experimental research may be a main reason. To answer these two phenomena, service performance of 15 RC beam specimens with uncoated and epoxy-coated reinforcements under different fatigue loads was experimentally studied. Influences of different coating thicknesses of the reinforcing bars, the fatigue load range and load upper limit as well as fatigue load cycles on the mechanical performance of RC test specimens are discussed. It is concluded that, for the test specimens subjected to the comparatively lower load range and load upper limit, adverse effect on the service performance of test specimens with thicker epoxy-coated reinforcing bars is negligible. With the increments of the coating thickness and the in-service loading level, i.e., fatigue load range, load upper limit and fatigue cycles, the adverse factor resulting from the thicker coating becomes noticeable.

Keywords: epoxy-coat bar; fatigue load; load upper limit; coating thickness; fatigue cycles

1. Introduction

To prevent the corrosion of the reinforcing bars in reinforced concrete (RC) structures exposed to aggressive environments, several methods of corrosion protection are commonly used. These include improving the quality of concrete and increasing cover thickness, providing a protective coating on the surface of concrete, using corrosion inhibitors, implementing cathodic protection and protecting the steel reinforcement in concrete. Among those protective measures, giving a durable and adhesive coating to the rebar is considered as a most feasible and cost-effective option from technical and economical view (Erdoğdu *et al.* 2001, Selvaraj *et al.* 2009).

In the past years, a large amount of research work on the bond performance of epoxy-coated rebars has been conducted (Johnston and Zia 1984, Treece and Jirsa 1989, Cleary and Ramirez 1991, Hamad *et al.* 1993, Cairns and Abdullah 1994, Cairns and Abdullah 1995, Hamad 1995, Castro 1996, Idun and Darwin 1999, Yeih *et al.* 2004, Anda *et al.* 2006). Because the surface of the reinforcing bar is coated by epoxy coating, the bond behavior between the reinforcing bar and the concrete may be influenced by the coating. For the smooth bars, the reduction in the friction coefficient is not statistically significant (Castro 1996); while for the ribbed bars, bond strength of the epoxy-coated bars is reduced by the epoxy coating (Cleary and Ramirez 1991, Cairns and Abdullah 1994, Castro 1996). The extent of the bond reduction of the epoxy-coated bars compared to that of the uncoated (normal) bars are related to several factors, such as the coating thickness (Treece and Jirsa 1989, Anda *et al.* 2006), depth of the concrete cover (Cairns and Abdullah 1994, Anda *et al.* 2006), rib parameters (Cairns and Abdullah 1994, 1995, Hamad 1995, Idun and Darwin 1999), confined reinforcements (Cairns and Abdullah 1994, Anda *et al.* 2006), the adopted bond test methods (Cairns and Abdullah 1994) and the type of the concrete (Yeih *et al.* 2004).

In addition, research work on the mechanical behaviour of the RC members containing epoxy-coated reinforcements at the serviceability and ultimate limit states has also been investigated (Cleary and Ramirez 1993, Cairns 1994, Kayyali and Yeomans 1995, Abrishami *et al.* 1995, Hasan *et al.* 1996). At characteristic service static load, the reduction in bond performance of reinforcements as a result of epoxy coating did influence the crack formation and the deflections of RC beams with epoxy-coated bars. For beams reinforced with ribbed bars, the ultimate capacity in flexure with epoxy coated steel was not significantly different to that of beams reinforced with black steel bars (Kayyali and Yeomans 1995). For normal and high-strength RC beams with epoxy-coated bars, lower ductility and wider crack

∗Corresponding author, Associate Professor
E-mail: w_xiaoh@163.com/Xiao-Hui.Wang@hw.ac.uk

http://www.techno-press.org/?journal=cac&subpage=8 ISSN: 1598-8198 (Print), 1598-818X (Online)

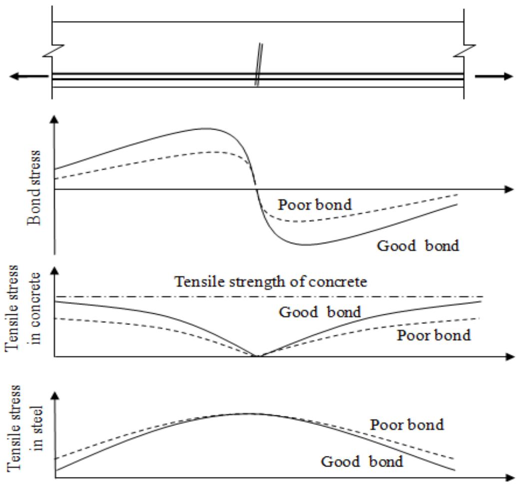

Fig. 1 Influence bond characteristics of reinforcement cracking and tension stiffening (Cairns 1994)

width were showed as compared to the corresponding beams with uncoated bars (Abrishami *et al.* 1995). For RC elements with epoxy-coated bars subjected to repeated loading (Cleary and Ramirez 1993, Hasan *et al.* 1996), in general, deflections, crack widths, and reinforcement stresses were larger in beams with epoxy-coated bars during service loading. During the repeated loading portion of the tests, the differences in crack widths, deflections, and bar stresses in beams with coated and uncoated bars were reduced with repeated loading (Cleary and Ramirez 1993), especially for the differences in deflections (Hasan *et al.* 1996).

Although it was reported that use of epoxy coated bars results in wider crack widths as compared to the corresponding beams with uncoated bars, field surveys always showed that the corrosion resistance of the epoxy-coated reinforcing bars is better than the uncoated bars (Venkatesan *et al.* 2006, Smith and Virmani 1996, Manning 1996, Weyers *et al.* 1997, Montes *et al.* 2004, Fanous and Wu 2005, Sohanghpurwala 2005, Cusson *et al.* 2008, Sagüés *et al.* 2010, Lau *et al.* 2010, Lawler *et al.* 2011). There is true even when there are signs of corrosion of the epoxy-coated reinforcing bars exhibited in the cracked zones (Smith and Virmani 1996, Montes *et al.* 2004). For the experimental research work carried out in the lab, the maximum service loads of the test specimens were used to study the mechanical behaviour of the RC members containing epoxy-coated reinforcement. This may be not a typical case for most in-service RC elements. For the corrosion behavior of epoxy-coated reinforcing bars in-service, it is influenced by both their in-service environments and external loads. In addition, the actual coating thicknesses of the epoxy-coated bars were seldom mentioned (Cleary and Ramirez 1993, Cairns 1994, Kayyali and Yeomans 1995, Abrishami *et al.* 1995, Hasan *et al.* 1996).

While there has been a fair amount of research done on performance of the RC elements with epoxy-coated reinforcing bars, it is still necessary to assess how the corrosion performance of RC members with epoxy-coated reinforcing bars was influenced by the in-service environments and the external loads; in addition, the influence of the actual coating thickness and level of in-service loading on their structural performance is still unclear.

In the present paper, the in-service mechanical behavior of the RC beam specimens containing epoxy-coated and uncoated reinforcements under different fatigue loads is mainly presented. In order to study how the service performance of the RC elements with epoxy-coated bars is influenced by different levels of in-service loads and the actual coating thicknesses of the epoxy-coated bars, 15 RC beams with uncoated and epoxy-coated reinforcements were experimentally loaded under different fatigue loads, where two peak fatigue loads and two fatigue loading cycles were considered. Influences of different coating thicknesses of the reinforcing bars, the fatigue load range and load upper limit as well as fatigue loading cycles on the mechanical performance of RC test specimens are discussed, taking into account the bond behavior of epoxy-coated reinforcing bar and tension stiffening under fatigue loading.

Experimental results of fatigue loading and the parameters discussion are mainly presented while the theoretical analysis models of RC test specimens under in-service loading and the corrosion behavior of the epoxy-coated and uncoated reinforcements in the test specimens will be reported in the following papers.

2. Theory

2.1 Bond behavior, tension stiffening and the crack width under monotonic loading

Bond behaviors of reinforcement influence the transfer of the force between reinforcing bar and concrete, and may affect structural performance in two ways: tension stiffening effect-the reduction in average bar strains between transverse cracks and the distance between successive transverse cracks. Usually, the stiffer the load/slip relationship, the more rapid the transfer of force, and the shorter the distance required to increase tensile stress in the concrete to the level at which a crack will form (Fig. 1) (Cairns 1994).

Thus, compared to the good bond in the ordinary uncoated reinforcing bar, the comparatively “poor bond” of the epoxy-coated bar may result in a lower tensile stress in concrete and higher tensile stress in steel (see Fig. 1) as well as longer distance between successive transverse cracks.

Under static monotonic loading, according to Eurocode 2, the maximum crack width w_k is given as (Walraven 2008)

$$w_k = s_{r,\max}(\varepsilon_{sm} - \varepsilon_{cm}) \tag{1}$$

Where $s_{r,\max}$ is the maximum crack distance, given as

$$s_{r,\max} = 3.4c + 0.425 \cdot k_1 \cdot k_2 \cdot \frac{d_b}{\rho_{p,eff}} \tag{2}$$

Where c is the concrete cover; d_b is the bar diameter; $\rho_{p,eff}$ is the effective reinforcement ratio; k_1 is the bond factor, 0.8 for high bond bars and 1.6 for bars with plain surface; k_2 is strain distribution coefficient. (ε_{sm}-ε_{cm}) is the difference in deformation between steel and concrete over the maximum crack distance, given as follows

$$(\varepsilon_{sm}-\varepsilon_{cm})=\frac{\sigma_s}{E_s}-\frac{k_t\cdot f_{ct,eff}\cdot\left(1+\alpha_e\cdot\rho_{p,eff}\right)}{E_s\cdot\rho_{p,eff}} \tag{3}$$

Where σ_s is the stress in the tension steel assuming a cracked section; E_s is the Young's modulus of steel, k_t accounts for the load duration; $f_{ct,eff}$ is the effective tensile strength of the concrete, α_e is the short-term modular ratio. The first part of the Eq. (3) accounts for the steel strain calculated on the basis of a fully cracked section and the second part effectively reduces the value of (ε_{sm}-ε_{cm}) by incorporating tension stiffening effects and strain within the concrete.

It should be pointed out that the change in bond characteristics may thus have a twofold influence on crack width, as crack spacing will be greater and tension stiffening less when bond stiffness is reduced. Coefficient k_1 in Eq. (2) takes account of bond properties, and is greater for bars with less stiff load-slip behaviour. The increase in k_1 is widely assumed to be inversely related to bond (fib 2000).

2.2 Local bond-slip under repeated loading

Pull-out test on the bond strength of uncoated reinforcing bars showed that, if fatigue failure does not take place in constant amplitude cycling loading, then the previous repeated load does not negatively influence the bond strength, compared with that of monotonic loading (Rehm and Eligehausen 1979), i.e., the slip values at the peak bond stresses do not vary much for various constant amplitude repeated loading while the slip and residual slip values increase with an increase of the number of load cycles (Oh and Kim 2007). The cycle dependent slip s_N can be expressed as a function of the initial slip s_1 by first cyclic loading and the number of load cycles N as shown

$$s_N=s_1\cdot N^b \qquad b=0.098 \tag{4}$$

For the bond behavior under fatigue loading, test results showed that, under bond fatigue loading in a working stress range, the slip behavior of the mill scale, epoxy coated and blast cleaned bars is essentially similar for a range of bar size; epoxy coated bar slip in the first cycle was greater than mill scale bar slip and these differences diminished as the number of cycles increased (Johnston and Zia 1984).

3. Experimental program

3.1 Specimens details

All test specimens were designed with a rectangular cross section of $b\times h$=300×120 mm (Fig. 2). The overall length of the specimen was about 1500 mm with 1100 mm distance between two supports. All the specimens were provided three 12 mm diameter deformed bars as flexural reinforcements. 8 mm-diameter smooth bars were used to serve as the distribution reinforcements. The 8 mm-diameter plain bars were uniformly spaced at 50 mm at the beam ends and 100 mm at the beam span, see Fig. 2. The clear concrete cover of the tensile bars is 40 mm to meet the requirement of the minimum concrete cover of the RC members in the chloride-contained environment (GB50010-2010 2010).

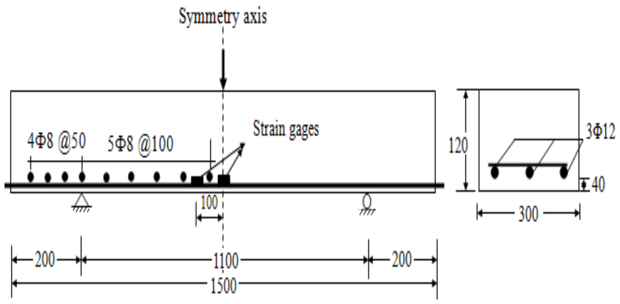

Fig. 2 RC test specimens

3.2 Materials

For the nominal diameter 12 mm and 8 mm reinforcing bars, two nominal coating thicknesses 200 μm and 600 μm were chosen, respectively. The coated and uncoated reinforcing bars were bought from OSD Company, where the epoxy coating process involves blast cleaning, preheating, electrostatic spray coating and curing in accordance with JG3042-1997 (1997). It was reported that all bars of the same size were from the same heat and all 12 mm bars had the same deformation pattern. Rib parameters of the 12 mm reinforcing bars and the actual coating thickness were measured to check the production quality of the epoxy coating. The actual coating thickness of 1500 mm beam length (see Fig. 2) was measured in accordance with JG3042-1997 (1997). The test was carried out using a coating thickness gauge.

12 mm reinforcing bars are the so-called hot-rolled ribbed steel bars HRB335 (Grade II), having standard yield strength of 335 MPa; while 8 mm reinforcing bars are hot-rolled plain steel bars HPB300 (Grade I) with standard yield strength of 300 MPa. The actual yielding strength, ultimate strength, modulus of elasticity and elongation of the coated and uncoated 12 mm reinforcing bars were measured to meet the required mechanical parameters.

Commercial concrete from the same batch was used to cast all the test specimens. The concrete had target strength of 40 Mpa. Portland cement PII 52.5 and coarse aggregate with maximum aggregate size of 25 mm were used in the concrete mixture. The slump of the concrete is 140±20 mm. Concrete mix proportion of the water:cement:sand: aggregate:superplasticizer:admixture=180:320:770:1020:4. 51:90 and the water-cement ratio is 0.44. The compressive strength of 150×150×150 mm concrete cube at 28 days was 50 MPa.

3.3 Fabricating of test specimens

For the RC specimens with uncoated reinforcing bars,

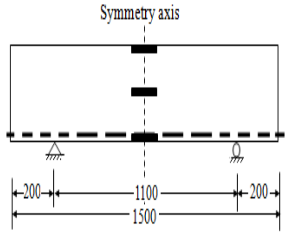

(a) The positive surface of the specimen

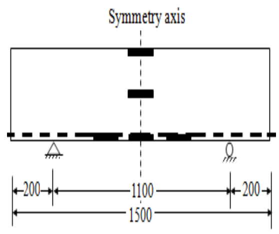

(b) The opposite surface of the specimen

Fig. 3 Strain gage positions on the two lateral surfaces of the test specimen

Fig. 4 Test setup and the pulse fatigue testing machine

thin steel wires were used to make the steel cages; while for the RC specimens with epoxy-coated reinforcing bars, nylon strings were used to prevent the possible damage of the epoxy coating. In order to provide detailed strain readings of the longitudinal tensile reinforcements during loading process, six strain gages were installed in the designed positions of two lateral longitudinal tensile reinforcements before the casting of the concrete, see Fig. 2.

At the structural laboratory, wood molds were used to horizontally cast the test specimens to minimize the variation of concrete strength. During the casting and vibrating the concrete, care was taken to protect the strain gages from damage. Companion concrete cubes 150×150×150 mm were also cast to determine the corresponding compressive strength of concrete.

3.4 Loading test

After 28-days of curing, test specimens were prepared for load testing. Strain gages on the concrete were installed to measure the concrete strains during the loading test (see Fig. 3). Then, RC test specimen was placed in the test set-up with both ends simply supported and a single, mid-span load point (Fig. 4). A 100 kN pulse fatigue testing machine was used to apply static and fatigue loading to the RC specimens (Fig. 4). The strains of the steel and concrete were recorded by a DH3817 dynamic strain data measurement system. Displacement at mid-span of the test specimen was measured at mid-depth of the section by a displacement transducer. Vertical displacements at the two supports were also measured by using displacement transducers placed on top surfaces of the test specimens (see Fig. 4). Support deformations were then subtracted from the mid-span displacement to determine the specimen deformation.

During all loading test, the magnitudes of static and fatigue loads were controlled and measured by a load cell. For the control RC specimens subjected to three-point static loading, fine sand was put under both ends of the specimens to overcome the unevenness of the specimens themselves. For the RC specimens subjected to three-point fatigue loading with 4 Hz frequency, the day before loading, the cement paste was used to fill the space between each end of the specimen and the underneath support to prevent shifting of the specimen on the supports during fatigue loading cycles. In order to study the mechanical performance of the RC specimens under service loads, test specimens were subjected to 500,000 cycles and 1,000,000 cycles, respectively.

At the beginning of the fatigue loading, test specimen was static-loaded to the upper limit of the fatigue load and developments of the cracks and the maximum crack widths at two lateral surfaces were recorded; then, this load was unload to zero and fatigue load was performed. For the test specimens subjected to 500,000 loading cycles, when the number of loading cycles reached 50,000, 100,000, 300,000 and 500,000, the fatigue loading was stopped and unloaded to zero; while for the test specimens subjected to 1,000,000 cycles, when the number of cycles reached 50,000, 100,000, 300,000, 500,000, 800,000 and 1,000,000, the fatigue loading was stopped and unloaded to zero. Then, during each fatigue loading stoppage, developments of the cracks were observed and the corresponding numbers of the load cycles were recorded at the cracking tips. Maximum cracking widths at two lateral surfaces were also measured by using a Digital Concrete Crack Width Gauge. And then, test specimen was reloaded to the upper limit of the fatigue load and the developments of the cracks and the maximum cracking widths were measured again.

4. Test results and discussion

4.1 Detailed results of the actual test specimens

The actual dimensions and the average clear concrete cover of the RC test specimens are summarized in Table 1, where four types of RC test specimens are listed. In Table 1, test specimens were identified with letters and numbers designation. For test specimens with uncoated reinforcing bars, letter “C” indicates control test specimens; letters “FE” indicate test specimen subjected to fagiue load and environment attack; letters “DE” indicate test specimen subjected to dead load and environment attack. For test specimens with epoxy-coated reinforcing bars, the first letter “E” indicates epoxy coating, including both tensile and distribution bars; the second numbers indicate 200 μm (0.2 mm) and 600 μm (0.6 mm) nominal coating thicknesses; the following letters “FE” or “DE” indicate fagiue load and environment attack or dead load and environment attack; the final number indicates the specimens number (As mentioned above, the experimental results of fatigue loading and the parameters discussion are mainly presented in the present paper. The loaded and unloaded test specimens are undergoing simulated seawater

Table 1 Details of the RC test specimens

RC test specimen		Length (mm)	Cross section (mm)		Average clear concrete cover (mm)	Coating thickness of the reinforcing bar in different position (μm)		
			Width	Height		Positive side (see Fig. 3)	Middle	Opposite side (see Fig. 3)
Control	C1	1502	301	120.5	40.0	0.0	0.0	0.0
	E0.2C1	1501	300	119	40.5	237.7 (55.1)	258.3 (56.4)	184.2 (38.2)
	E0.6C1	1500	301	120.5	40.0	661.6(106.0)	673.0(115.1)	792.6(133.6)
Fatigue group 1: 500,000 cycles and fatigue load 1	FE1	1501	299	118	40.0	0.0	0.0	0.0
	E0.2FE3	1502	302	119.5	40.0	245.9 (65.5)	225.9 (63.7)	214.9 (43.9)
	E0.2FE6	1501	300	120	40.5	306.3 (71.8)	193.2 (53.3)	216.6 (33.9)
	E0.6FE3	1501	300	120.5	40.0	1054.7(191.0)	984.1(116.2)	667.7(104.5)
	E0.6FE4	1500	301	121.5	40.0	864.1(141.1)	691.1(101.4)	745.3(130.6)
Fatigue group 2: 500,000 cycles and fatigue load 2	FE2	1504	300	119.5	40.5	0.0	0.0	0.0
	E0.2DE2	1500	303	120	40.5	274.8(183.7)	361.8 (83.8)	323.5 (66.8)
	E0.2FE5	1500	300	120.5	40.5	213.5 (42.0)	225.9 (60.5)	230.0 (76.0)
	E0.6FE5	1501	300	121.5	41.0	492.9(59.1)	711.1(145.2)	677.6(121.3)
	E0.6DE1	1503	302	119.5	41.0	522.0(122.7)	524.9(161.7)	578.8(72.3)
Fatigue group 3: 1,000,000 cycles and fatigue load 2	DE2	1500	304	120.0	40.5	0.0	0.0	0.0
	E0.2FE1	1501	301	120	40.5	214.3 (69.0)	246.2 (61.1)	242.6 (77.1)
	E0.2FE2	1502	301	120	40.5	364.6 (73.1)	317.2 (50.7)	292.2 (53.8)
	E0.6FE1	1502	300	121.5	40.5	528.3(124.0)	945.2(105.0)	800.7(147.6)
	E0.6DE2	1500	302	120.5	40.5	766.9(109.7)	707.2(161.1)	649.1(154.9)

Table 2 Mechanical test results of the uncoated and coated reinforcing bars

12 mm deformed bar	Actual coating thickness (μm)	Modulus of elasticity (GPa)	Elongation (%)	Yielding strength (MPa)	Ultimate strength (MPa)
uncoated	0.0	181	19.0	367.8	541.9
200 μm nominal coating thickness	a, 251.3 (80.3)	173	16.3	390.8	590.1
	b, 299.9 (126.1)	198	17.5	395.3	604.8
	c, 287.9 (107.9)	180	17.9	382.0	592.4
600 μm nominal coating thickness	a, 755.8 (184.8)	197	17.2	370.5	556.2
	b, 705.8 (129.2)	189	18.1	360.8	549.1
	c, 1078.4 (96.5)	194	17.1	374.1	557.1

solutions attack now and the test results of the corrosion performance of the test specimens will be reported later). For example, test specimen FE2 indicates RC specimen with uncoated reinforcing bars subjected to fagiue load and environment attack; test specimen E0.2FE6 indicates RC specimen with epoxy-coated reinforcing bars, where both tensile and distribution bars have 200 μm nominal coating thickness. It should be pointed out, during the loading test, in order to ensure the better conditions of the test specimens subjected to fatigue loads, some test specimens originally used in the static loading were exchanged and used in the fatigue loading test, for instance, test specimens DE2, E0.2DE2, E0.6DE1 and E0.6DE2. The detailed information for fatigue loading 1 and loading 2 will be determined in the later section 4.4.

For three 12 mm coated bars used in each specimen, the average coating thickness and standard deviation (the number in the bracket) of each reinforcing bar are showed in Table 1. For 12 mm ribbed reinforcing bar, it has core diameter of 11.45(0.094) mm, height of one longitudinal rib of 0.98(0.058) mm and height of one transverse rib of 0.93(0.148) mm. For some 12mm reinforcing bars with 600 μm nominal epoxy coating, the actual coating thickness of the bar is larger than the rib heights resulting in the reduction of the relative rib area value, this may influence the bond behavior of the epoxy-coated bar under loads, as pointed out by Anda *et al.* (2006) and Fei and Darwin (1999). For each epoxy-coated reinforcing bar, along its 1500 mm length, the coating thicknesses are not uniform. For reinforcing bars with thinner coating, this situation is better than the reinforcing bars with thicker coating. Very heavy coating thickness is often observed along the two longitudinal ribs of the reinforcing bar with 600 μm nominal coating thickness, making space around the longitudinal rib very smooth.

4.2 Mechanical test results of the uncoated and coated reinforcing bars

Mechanical test results of the actual yielding strength, ultimate strength, modulus of elasticity and elongation of the coated and uncoated 12 mm reinforcing bars are shown in Table 2. The nominal diameter of the 12 mm was used to determine the nominal area of the deformed bar. It can be seen from Table 2 that the measured mechanical parameters are quite good, meeting the required ones of 12 mm reinforcing bars (HRB335, Grade II).

For the epoxy-coated reinforcing bars, due to the high temperature (about 230℃) during the electrostatic spray process of the epoxy coating on the surface of the reinforcing bar, the yielding strength, ultimate strength and modulus of elasticity of the coated bars are higher than those of the uncoated reinforcing bars with the same nominal diameter; while the elongation of the coated reinforcing bars is lower than that of the uncoated reinforcing bars. Those differences reduce with the increase of the coating thickness, see Table 2.

4.3 Test results of control test specimens

Control RC test specimens C1, E0.2C1 and E0.6C1 (detailed information of those specimens can be seen in Table 1) were statically loaded to fail in order to determine the fatigue load range. For three control specimens, the tensile bars firstly yielded then the specimens failed in crushing of the concrete in the compressive zone. The load-deflection curves of three control RC test specimens is shown in Fig. 5, where in Fig. 5, the shorter load-deflection curve of test specimen C1 resulted from the earlier removal of the displacement transducers. The loads of three test specimens

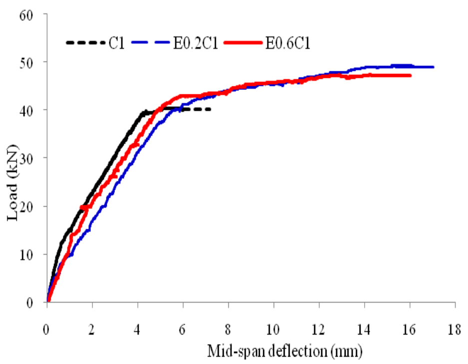

Fig. 5 Load-deflection curves of three control RC test specimens

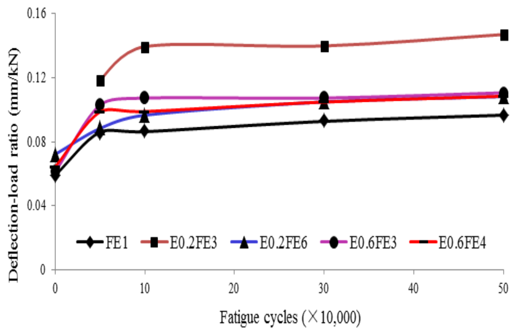

Fig. 6 Deflection-load ratio versus fatigue cycles of test specimens in fatigue group 1

Table 3 Comparison of the loads at different phases and the average spacing of the main failure cracks of three test specimens

Test specimen	Cracking load (kN)	Yielding load (kN)	Ultimate load (kN)	Load when the maximum crack width reaches 1.5 mm (kN)	Average spacing of the main failure cracks (mm)
C1	5.0	39.6	47.3	41.3	111.7
E0.2C1	5.1	40.9	49.4	45.4	120.0
E0.6C1	5.0	43.5	47.3	45.6	146.0

at different phases and the average spacing of the main failure cracks are shown in Table 3.

It can be seen from Fig. 5 and Table 3 that, the cracking loads of the control test specimens are little influenced by the epoxy coating and the coating thicknesses. Before the appearance of the cracks, the load-deflection curves of three control RC test specimens are almost identical. During the range of cracking load to yielding load, under the same load, the smallest mid-span deflection is observed in specimen C1 while the largest one is presented in specimen E0.2C1. Due to the higher yielding and ultimate strength of the coated reinforcing bars (see Table 2), yielding and ultimate loads of test specimens E0.2C1 with thinner coated bars are higher than those of the test specimen C1 with uncoated bars, while the ultimate load of test specimens E0.6C1 is nearly identical to that of the test specimen C1. Those test results slightly differs from the test results of Abrishami *et al.* (1995), where it was reported that the ultimate capacity in flexure of beams with epoxy coated steel was not significantly different to that of beams reinforced with black steel bars. However, it should be pointed out that the actual coating thicknesses and the yielding strength of the coated bars in experiment of Abrishami *et al.* (1995) were unknown.

The ratios of the yielding load to ultimate load of the specimens C1, E0.2C1 and E0.6C1 are 0.837, 0.830 and 0.920, respectively, showing less ductility in specimen E0.6C1 with thicker coating (average coating thickness of three tensile bars is 700 μm, see Table 1). For specimen E0.2C1 with thinner coating (average actual coating thickness 226 μm of three tensile bars, see Table 1), the ductility is even slightly larger than the uncoated one. Due to the comparatively "poor bond" of the epoxy-coated reinforcing bar (see Fig. 1), wider average spacing of the main failure cracks is also observed in test specimens E0.2C1 and E0.6C1 in Table 3, especially for E0.6C1 with thicker coating. Similar results were also reported by Cleary and Ramirez (1991).

4.4 Determining the fatigue load range

Considering the following factors to determine the load range of the fatigue loading test: a) The upper stress limit 0.6 f_y of the RC elements under service loads, where f_y is the yield strength of the tensile reinforcing bar (Cleary and Ramirez 1993, Hasan *et al.* 1996), b) For the RC element subjected to fatigue load, the range of the maximum fatigue loading is about 35%-57% of the yield load of the RC element; c) The cracking load of the control RC test specimens (see Table 3), the loading ranges of fatigue loading 1 and fatigue loading 2 in Table 1 were determined, where the loading ranges of fatigue loading 1 and loading 2 are 5.4-18 kN and 2.8-14 kN, respectively. The maximum fatigue loads 18 kN and 14 kN are about 41%-45% and 32%-35% of the yield load of the control RC test specimens, respectively.

4.5 Test results of fatigue group 1

In fatigue group 1, the RC specimens were subjected to 500,000 loading cycles and 5.4-18 kN fatigue load. The mid-span deflection-load ratio versus fatigue cycles, the maximum increment of steel strain versus fatigue cycles and maximum increment of concrete strain in extreme edge of compressive zone versus fatigue cycles in test specimens of group 1 are shown in Figs. 6-8, respectively. As mentioned above, when the fatigue cycles reached the designated number of cycles, the fatigue load was unloaded to zero and static reloading to upper limit of the fatigue load was performed. The changes of the functioning steel strain gages (one/two strain gages were damaged during the load testing) in six positions (see Fig. 2) and concrete strain gages in the extreme edge of the positive and opposite surfaces (see Fig. 3) before and after each static loading (i.e., fatigue loading stoppage) were recorded and the largest differences among the functioning steel strains and concrete strains are defined as the maximum increment of steel strain and maximum increment of concrete strain, respectively. The maximum increment of steel strain changes with the fatigue cycles, reflecting crack development at different times during the

Table 4 Developments of maximum crack widths at the two lateral surfaces of the test specimens in fatigue group

Fatigue cycles (×10,000)	Loading condition	$w_{c,\ max}$ (mm)									
		FE1		E0.2FE3 (+)		E0.2FE6		E0.6FE3		E0.6FE4	
		$w^P_{c,\max}$	$w^O_{c,\max}$	$w^P_{c,\max}$	$w^O_{c,\max}$	$w^P_{c,\max}$	$w^O_{c,\max}$	$w^P_{c,\max}$	$w^O_{c,\max}$	$w^P_{c,\max}$	$w^O_{c,\max}$
0	loading	—	—	0.25	0.2(*)	0.06	0.08	0.2	0.25	0.2	0.25
	unloading			—	—	—	—	0.1	0.1	0.05	0.05
5	unloading	0.06	0.1	0.2	0.2(*)	0.1	0.1	—	—	0.1	0.1
	loading	0.2	0.2	0.3	0.3(*)	0.2	0.15	0.3	0.25	0.2	0.25
10	unloading	0.1	0.1	0.2	0.15(*)	0.15	0.15	0.2	0.25	0.18	0.2
	loading	0.2	0.2	0.35	0.3(*)	0.2	0.2	0.3	0.32	0.25	0.25
30	unloading	0.1	0.1	0.1	0.22(*)	0.15	0.15	0.2	0.25	0.2	0.2
	loading	0.25	0.22	0.35	0.35(*)	0.25	0.25	0.3	0.35	0.3	0.32
50	unloading	0.25	0.2	0.18	0.2(*)	0.15	0.15	0.25	0.25	0.2	0.15
	loading	0.32	0.32	0.35	0.35(*)	0.25	0.25	0.35	0.35	0.3	0.35

Note: (*) indicats initial crack before loading; (+) indicats test specimen with a 60 mm length crack in the opposite surface before loading, resulting from the transporting damage

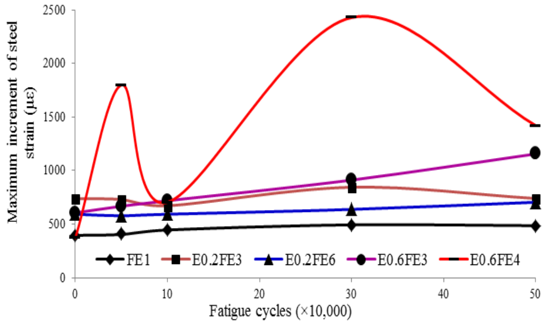

Fig. 7 Maximum increment of steel strain versus fatigue cycles of test specimens in fatigue group 1

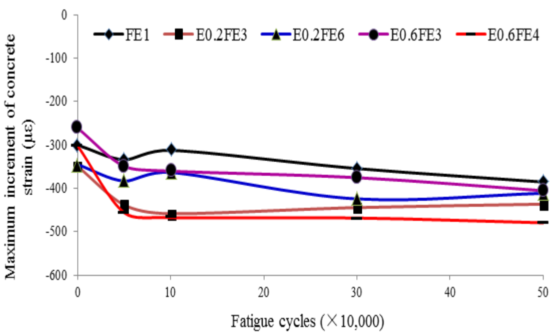

Fig. 8 Maximum increment of concrete strain in extreme edge of compressive zone versus fatigue cycles of test specimens in fatigue group 1

loading test and the corresponding stress redistribution of the tensile reinforcing bars in the test specimen. The developments of maximum crack widths at the two lateral surfaces with the fatigue cycles are shown in Table 4, where $w^P_{c,max}$ and $w^O_{c,max}$ are the maximum crack widths at the positive and opposite surfaces, respectively.

It can be seen from Fig. 6 that, during the whole loading cycles, the RC test specimens with epoxy-coated reinforcing bars have larger mid-span deflection-load ratio than those of the test specimen FE1 with uncoated reinforcing bars. Similar test results were also obtained by Cleary and Ramirez (1993), where nearly maximum service loads of the test specimens were used as the fatigue load upper limit. The mid-span deflection-load ratio of five test specimens all increases with the fatigue load cycles due to the accumulation of slip with the increase of the repetition of load cycles, as indicated in Eq. (4). Larger increment of mid-span deflection-load ratio is observed before the 50,000 cycles, especially for specimens E0.6FE3 and E0.6FE4 with thicker coating and poor bond between the epoxy-coated bar and concrete. During 100,000 cycles to 500,000 cycles, slightly differences in the mid-span deflection-load ratio of five test specimens is presented in Fig. 6, indicating the decreased influence of the fatigue load on the local bond-slip with the increase of load cycles for both coated and uncoated reinforcing bars (Johnston and Zia 1984). Due to the initial crack located in the opposite surface before loading, the specimen E0.2FE3 has a largest mid-span deflection-load ratio, see Fig. 6.

For five test specimens in this group, the maximum increment of steel strain increases with the increased number of cycles (Fig. 7), indicating the tension stiffening decay with the increases of loading cycles for RC test specimens containing uncoated and epoxy-coated reinforcing bars. Due to the poor bond in test specimens containing epoxy-coated bars, tension stiffening decays rapidly in the test specimens with thicker epoxy coating as compared with that in uncoated RC test specimen, resulting in larger reinforcement stresses in test specimens with epoxy-coated reinforcing bars, as pointed out by Cleary and Ramirez (1993) and shown in Fig. 1. The largest increment of tensile strain (also the largest tensile strain) is observed in test specimen E0.6FE4, where the maximum crack widths were presented just near the symmetry axis at the two lateral surfaces and maximum tensile strains 2340 $\mu\varepsilon$ and 3271 $\mu\varepsilon$ were shown during the static loading after 50,000 and 300,000 fatigue cycles. This large increment in tensile strain at reinforcement level is mainly due to the opening and the propagation of these two cracks with

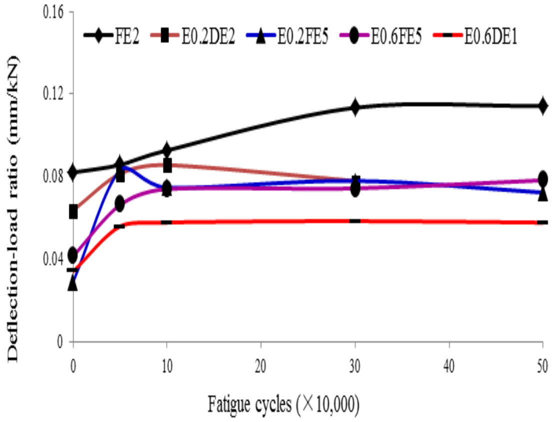

Fig. 9 Deflection-load ratio versus fatigue cycles of test specimens in fatigue group 2

maximum crack widths. At the end of 500,000 cycles, the residual tensile strain of reinforcing bar in this mid-span position is still very high, about 1685 $\mu\varepsilon$.

Fig. 8 shows all five specimens experienced a continual increase in compressive concrete strain with the increase of load cycles. The largest increment of concrete strain in extreme edge of compressive zone is also observed in test specimen E0.6FE4 with thicker epoxy coating.

The maximum crack widths at the two lateral surfaces of the test specimens increases with the increased fatigue cycles (see Table 4). At the beginning at the fatigue load (0 fatigue cycles), two test specimens E0.6FE3 and E0.6FE4 have wider cracks than test specimen E0.2FE6. This is mainly due to different bond conditions among the three specimens since other parameters in the test specimens are same, see Eq. (1). Before the 100,000 cycles, due to the initial larger slip resulting from the poor bond condition, specimens with epoxy-coated reinforcing bars have larger crack widths than that of the specimen FE1 with uncoated reinforcing bar. However, this difference in crack width decreases with increased number of cycles. This may result from the decrease of the slip difference between the uncoated and coated bar as the number of cycles increased (Johnston and Zia 1984). Similar phenomenon was also observed by Cleary and Ramirez (1991).

4.6 Test results of fatigue group 2

In fatigue group 2, RC test specimens were subjected to 500,000 loading cycles and 2.8-14 kN fatigue load. The mid-span deflection-load ratio versus fatigue cycles, the maximum increment of steel strain versus fatigue cycles and maximum increment of concrete strain in extreme edge of compressive zone versus fatigue cycles in test specimens of group 2 are shown in Figs. 9-11, respectively. The lack of data in Figs. 9 and 11 resulted from the damage of the some concrete and/or steel strain gages, earlier removal of the displacement gages before the starting of the fatigue loading and experimental errors. For test specimen FE2, it had an initial crack in the loading surface; while for specimen E0.6DE1, it had an initial crack in the positive surface, extending 45° along the whole height of the test specimen.

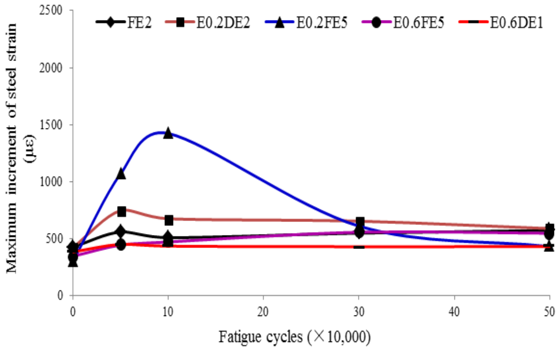

Fig. 10 Maximum increment of steel strain versus fatigue cycles of test specimens in fatigue group 2

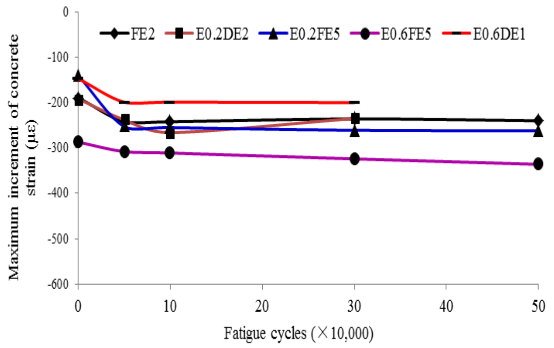

Fig. 11 Maximum increment of concrete strain in extreme edge of compressive zone versus fatigue cycles of test specimens in fatigue group 2

For the test specimens in fatigue group 2, although they were subjected to the same loading cycles as those in fatigue group 1, due to the lower fatigue load range and lower fatigue load upper limit, the situation is quite different. For the mid-span deflection-load ratio versus fatigue cycles shown in Fig. 9, the specimen FE2 with uncoated reinforcing bars has the largest one while the specimen E0.6DE1 with coated reinforcing bars (600 μm nominal coating thickness and average 542 μm actual coating thickness of three tensile bars) has the lowest one, indicating that the fatigue load range and magnitude of the load upper limit may be key factors influencing the service performance of the test specimens with coated reinforcing bars regardless of both specimens having initial cracks. Due to the similar reason as presented in specimen E0.6FE4 shown in Fig. 7, the largest increment of tensile strain is observed in test specimen E0.2FE5 (see Fig. 10), which also presents larger mid-span deflection increment from loading initiation to 50,000 cycles. Although the obvious increment in steel strain is showed before 50,000 cycles for five test specimens in this group, this increment decreases during 50,000 cycles to 100,000 cycles and becomes nearly stabile, indicating the tension stiffening decay within the 50,000 cycles and stabile tension stiffening after 100,000 cycles for test specimens containing uncoated and coated reinforcing bars. As a result, the maximum increment of steel strain in fatigue group 2 approaches after 500,000 cycle and 400-600 $\mu\varepsilon$ residual tensile strains of reinforcing bars are presented (Fig. 10), unlike the situation in Fig. 7. The situation in Fig. 11 is also different from that in Fig. 8. The maximum

Table 5 Development of maximum crack widths at the two lateral surfaces of the test specimens in fatigue group 2

Fatigue cycles (×10,000)	Loading condition	$w_{c,\ max}$ (mm)									
		FE2 (+)		E0.2DE2		E0.2FE5		E0.6FE5		E0.6DE1(+)	
		$w^P_{c,\max}$	$w^O_{c,\max}$	$w^P_{c,\max}$	$w^O_{c,\max}$	$w^P_{c,\max}$	$w^O_{c,\max}$	$w^P_{c,\max}$	$w^O_{c,\max}$	$w^P_{c,\max}$	$w^O_{c,\max}$
0	loading	0.14	0.06	0.2	0.12	0.1	0.02	0.26	0.2	0.22(*)	0.16
	unloading	—	—	—	—	—	—	—	—	—	—
5	unloading	0.12	0.08	0.14	0.14	0.1	0.06	0.2	0.2	0.25(*)	0.22
	loading	0.25	0.15	0.26	0.24	0.2	0.1	0.32	0.30	0.32(*)	0.24
10	unloading	0.10	0.06	0.12	0.13	0.1	0.06	0.2	0.16	0.22(*)	0.22
	loading	0.25	0.15	0.3	0.24	0.2	0.1	0.3	0.26	0.36(*)	0.32
30	unloading	0.1	0.06	0.20	0.18	0.1	0.06	0.24	0.2	0.2(*)	0.2
	loading	0.25	0.15	0.28	0.26	0.22	0.1	0.36	0.32	0.36(*)	0.3
50	unloading	0.1	0.06	0.18	0.16	0.06	0.06	0.24	0.2	0.2(*)	0.2
	loading	0.25	0.2	0.28	0.24	0.12	0.1	0.36	0.32	0.36(*)	0.32

Note: (*) indicats cracking with initial crack before loading; (+) indicats test specimen with initial cracking resulting from transporting damage

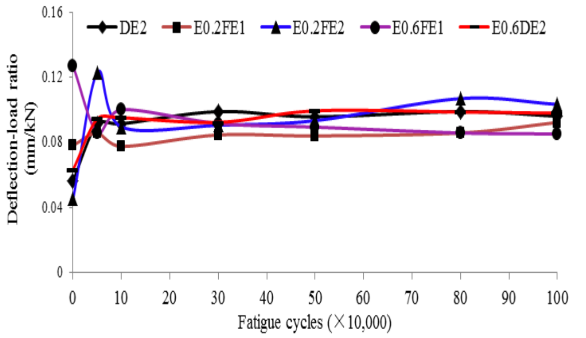

Fig. 12 Deflection-load ratio versus fatigue cycles of test specimens in fatigue group 3

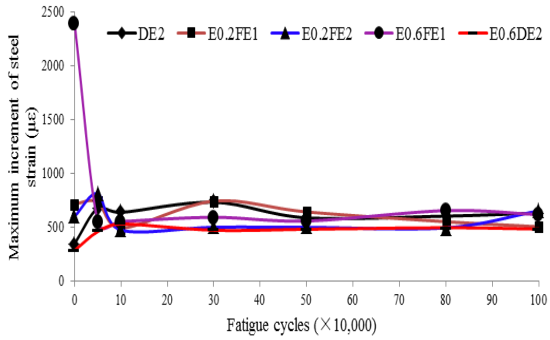

Fig. 13 Maximum increment of steel strain versus fatigue cycles of test specimens in fatigue group 3

increment of concrete strain in extreme edge of compressive zone in Fig. 11 lies in -200–-350 $\mu\varepsilon$ while this range is -350--500 $\mu\varepsilon$ in Fig. 8. Only in test specimen E0.6FE5 with the thickest epoxy coating in this group, the continual increase in compressive strain with the increase of load cycles is presented.

The developments of maximum crack widths at the two lateral surfaces with the fatigue cycles are shown in Table 5, where $w^P{}_{c,max}$ and $w^O{}_{c,max}$ are the maximum crack widths at the positive and opposite surfaces, respectively. Similar to the situation in Table 4, test specimens E0.6FE5 and E0.6DE1 with thicker nomial coating thickness have wider crack width than test specimens E0.2FE5 and E0.2DE2 with thinner nominal coating thickness. For 200 μm nominal coated test specimens E0.2DE2 (average 320 μm actual coating thickness of three tensile bars) and E0.2FE5 (average 224 μm actual coating thickness of three tensile bars), compartively wider crack widths are observed in specimen E0.2DE2 with compartively thicker coating thickness. However, for 600 μm nominal coated test specimens E0.6FE5 (average 627 μm actual coating thickness of three tensile bars) and E0.6DE1 (average 542 μm actual coating thickness of three tensile bars), neglecting the larger crack width resulting from the initial crack, at the later stage of fatigue cycles, the developing of the maximum crack widths of the two specimens are nearly identical, unlike the situation in Table 4, where test specimen E0.2FE3 with initial crack always has larger crack width than specimen E0.2FE6 without initial crack at each fatigue cycle.

4.7 Test results of fatigue group 3

In fatigue group 3, the RC specimens were subjected to 1,000,000 loading cycles and 2.8-14 kN fatigue load. The mid-span deflection-load ratio versus fatigue cycles, the maximum increment of steel strain versus fatigue cycles and maximum increment of concrete strain in extreme edge of compressive zone versus fatigue cycles in test specimens of group 3 are shown in Figs. 12-14, respectively. The lack of data in Fig. 14 resulted from the damage of the concrete strain gages. The developments of maximum crack widths at the two lateral surfaces with the fatigue cycles are shown in Table 6, where $w^P{}_{c,max}$ and $w^O{}_{c,max}$ are the maximum crack widths at the positive and opposite surfaces, respectively. For test specimen E0.6DE2, it had an initial crack in the right side of the positive surface, vertically extending about 60 mm long.

Table 6 Developments of maximum crack widths at the two lateral surfaces of the test specimens in fatigue group 3

Fatigue cycles (×10,000)	Loading condition	$w_{c,\ max}$ (mm)									
		DE2		E0.2FE1		E0.2FE2		E0.6FE1		E0.6DE2($^{+}$)	
		$w^{P}_{c,\max}$	$w^{O}_{c,\max}$	$w^{P}_{c,\max}$	$w^{O}_{c,\max}$	$w^{P}_{c,\max}$	$w^{O}_{c,\max}$	$w^{P}_{c,\max}$	$w^{O}_{c,\max}$	$w^{P}_{c,\max}$	$w^{O}_{c,\max}$
0	loading	0.1	0.1	0.1	0.1	0.2	0.15	0.28	0.14	0.24(*)	0.2
	unloading	—	—	—	—	—	—	—	—	—	—
5	unloading	0.08	0.1	0.12	0.08	0.16	0.1	0.2	0.2	0.1	0.1
	loading	0.15	0.2	0.18	0.18	0.24	0.22	0.3	0.3	0.2	0.2
10	unloading	0.08	0.1	0.08	0.1	0.2	0.15	0.24	0.2	0.26(*)	0.14
	loading	0.18	0.15	0.2	0.22	0.25	0.25	0.32	0.3	0.3(*)	0.22
30	unloading	0.1	0.12	0.1	0.1	0.1	0.08	0.2	0.18	0.2(*)	0.14
	loading	0.2	0.15	0.2	0.24	0.22	0.18	0.3	0.3	0.28(*)	0.22
50	unloading	0.1	0.1	0.15	0.12	0.15	0.1	0.2	0.2	0.22(*)	0.14
	loading	0.2	0.2	0.2	0.2	0.2	0.15	0.32	0.3	0.32(*)	0.22
80	unloading	0.1	0.1	0.1	0.1	0.14	0.14	0.24	0.2	0.26(*)	0.14
	loading	0.15	0.15	0.2	0.2	0.24	0.2	0.34	0.3	0.3(*)	0.22
100	unloading	0.1	0.1	0.1	0.1	0.14	0.12	0.2	0.2	0.26(*)	0.14
	loading	0.2	0.2	0.2	0.22	0.22	0.2	0.34	0.32	0.3(*)	0.22

Note: (*) indicats cracking with initial crack before loading; (+) indicats test specimen with initial cracking resulting from transporting damage

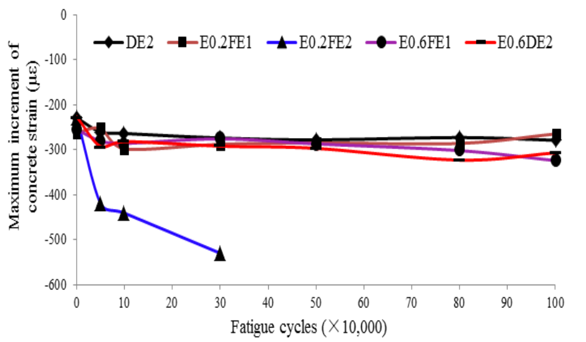

Fig. 14 Maximum increment of concrete strain in extreme edge of compressive zone versus fatigue cycles of test specimens in fatigue group 3

For the test specimens in fatigue group 3, the situations are similar to those in fatigue group 2 subjected to the same fatigue load range and load upper limit. For the mid-span deflection-load ratio of five test specimens, due to cracks were initialized at the symmetry axis at the two lateral surfaces, the largest increment of steel strain and largest mid-span deflection-load ratio are presented in specimen E0.6FE1. However, after the first 50,000 loading cycles, the mid-span deflection-load ratios and maximum increment of steel strains of five test specimens approach, see Fig. 12 and Fig. 13. Except for the test specimen E0.2FE2, the maximum increment of concrete strain in extreme edge of the other four specimens ranges from -250 $\mu\varepsilon$ to -350 $\mu\varepsilon$ (see Fig. 14), slightly larger than the concrete strain range shown in Fig. 11.

For the maximum crack widths at the two lateral surfaces shown in Table 6, with the increment of loading cycles, the crack widths of the test specimens with coated reinforcing bars become larger than those of the specimen DE2 with uncoated reinforcing bars. Similar to the situation in Table 4 and Table 5, test specimens E0.6FE1 and E0.6DE2 with 600 μm nomial coating thickness have wider crack width than test specimens E0.2FE1 and E0.2FE2 with 200 μm nomial coating thickness. The largerst crack widths at two lateral surfaces are presented in specimen E0.6FE1, which has the thickest average coating thickness 758 μm in group 3. For specimen E0.6DE2 with initial crack in the positive surface, the maximum crack width in this surface is increased by the initial crack before 50,000 loading cycle; with the increment of the loading cycles, the influence of the initial crack on the increment of the maximum crack width decreases.

5. Discussion of variables

5.1 Effect of different coating thicknesses on average maximum crack width of RC test specimens

For epoxy-coated test specimens in three fatigue groups 1-3, comparison of the average maximum crack widths at the lateral surface $w_{c,max}$ (mm) at unloading and loading states is shown in Fig. 15. At most cases, for test specimens in the same fatigue groups, as mentioned above, due to the poor bond condition between the epoxy-coated bar and concrete, test specimens with the thickest coating in each group have wider average maximum crack width in the lateral surface, see Fig. 15(c)-(f). For test specimens E0.2FE6, E0.6FE3 and E0.6FE4 without any initial damage in group 1, wider crack widths are presented in specimens E0.6FE3 and E0.6FE4 with thicker coating (average 902 μm and 767

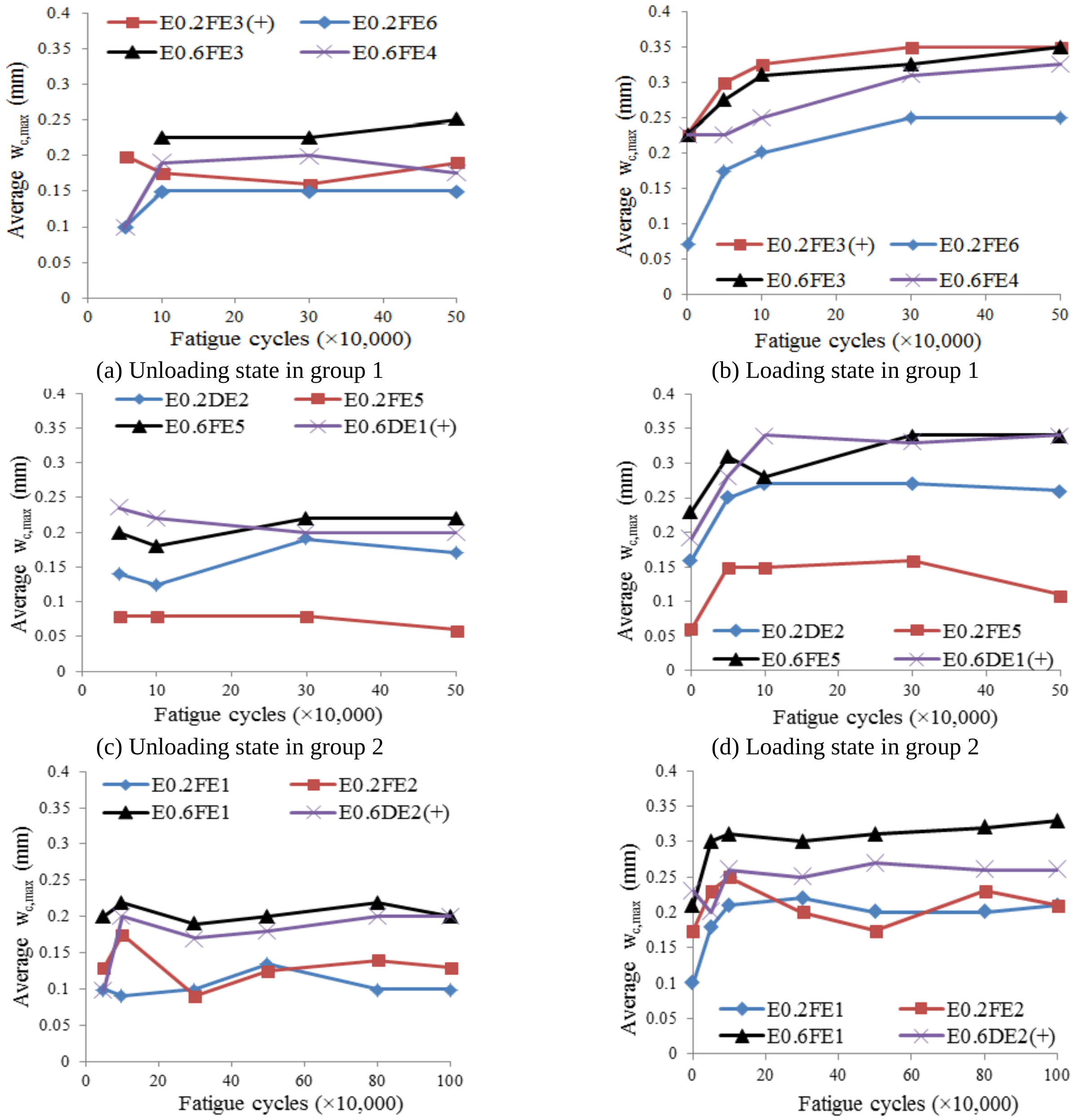

(a) Unloading state in group 1 (b) Loading state in group 1

(c) Unloading state in group 2 (d) Loading state in group 2

(e) Unloading state in group 3 (f) Loading state in group 3

Fig. 15 Comparison of average $w_{c,max}$ at lateral surface of epoxy-coated test specimens in groups 1-3

μm actual coating thickness for E0.6FE3 and E0.6FE4, respectively), see Fig. 7 and Fig. 15(a)-(b). Due to the same reason, in group 2, test specimen E0.6FE5 with thicker coating (average 627 μm actual coating thickness) has wider maximum crack widths in the two lateral surface than that of the test specimens E0.2DE2 and E0.2FE5 with thinner coating (average 320 μm and 224 μm actual coating thickness for E0.2DE2 and E0.2FE5, respectively); in group 3, test specimen E0.6FE1 with thicker coating (average 758 μm actual coating thickness) also has wider maximum crack widths. For coated test spcimens with initial cracks before loading, for instance, specimen E0.2FE3 in group 1, due to the developing of the initial crack into the maximum crack in the opposite surface, under loading states of 0, 50,000, 100,000, 300,000 and 500,000 fatigue cycles, the largest average maximum crack widths $w_{c,max}$ (mm) is presented in this specimen, see Fig. 15(b).

So, it can be concluded that, for epoxy-coated test specimens without any initial cracks before loading, when they are subjected to the same fatigue load (same fatigue load range and load upper limit as well as loading cycles), at both unloading and loading states, compartively wider maximum crack widths are presented in test specimens with thicker epoxy coating thickness.

5.2 Effect of different fatigue loads on the service performance of RC test specimens

For uncoated test specimens, E0.2 test specimens (i.e., 200-μmepoxy coating) and E0.6 test specimens (i.e., 600-μmepoxy coating) in three groups, comparison of the absolute mid-span deflections (mm) versus fatigue cycles is

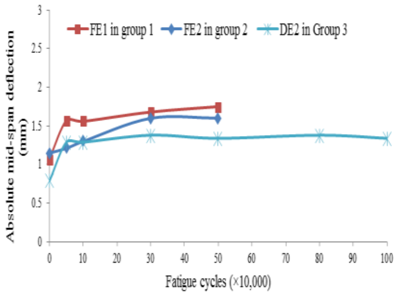

(a) Comparison of the absolute mid-span deflections for uncoated test specimens in three groups

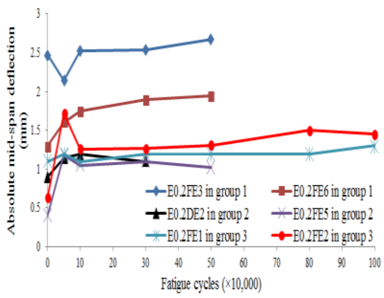

(b) Comparison of the absolute mid-span deflections for E0.2 coated test specimens in three groups

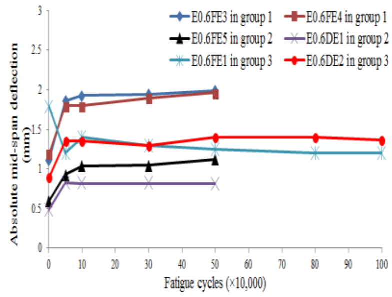

(c) Comparison of the absolute mid-span deflections for E0.6 coated test specimens in three groups

Fig. 16 Comparison of the absolute mid-span deflections for test specimens with different types of bars

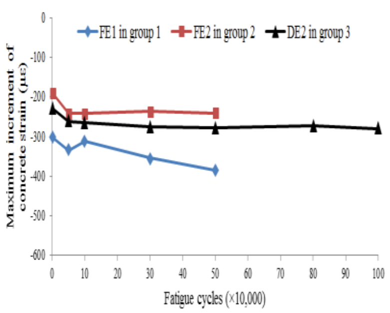

(a) Comparison of maximum increment of concrete strains for uncoated test specimens in three groups

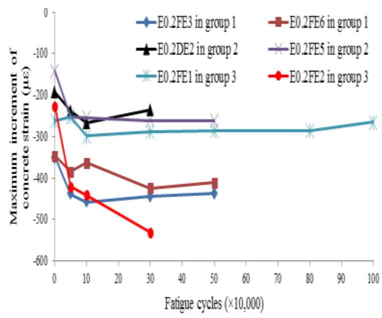

(b) Comparison of maximum increment of concrete strains for E0.2 coated test specimens in three groups

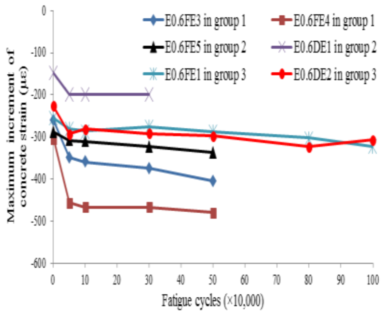

(c) Comparison of maximum increment of concrete strains for E0.6 coated test specimens in three groups

Fig. 17 Comparison of maximum increment of concrete strains for test specimens with different types of bars

shown in Fig. 16. It can be seen from Fig. 16 that, for each type of test specimens, due to the larger fatigue load range in fatigue group 1, where the load upper limit is about 41%-45% of the yield load of the control RC test specimens, larger absolute mid-span deflections are presented in test specimens of fatigue group 1. Due to the initial crack of FE2 before loading, test specimen FE2 in group 2 has larger mid-span deflection than that of the specimen FE1 at 0 fatigue cycles while larger mid-span deflection is presented in specimen FE1 in the following loading cycles, see Fig. 16(a). As mentioned above, due to the largest increment of steel strain and the cracks initiation locations at the symmetry axis of the two lateral surfaces, the largest mid-span deflection is presented in specimen E0.6FE1 at 0 fatigue cycles among the E0.6 test specimens (see Fig. 16(c)). However, in the following loading cycles, larger absolute mid-span deflections are also presented in test specimens of fatigue group 1.

Similarly, for each type of test specimens, i.e., uncoated specimens, E0.2 specimens and E0.6 test specimens in three groups, in most cases, larger increment of concrete strain in extreme edge of compressive zone is also shown in test specimens of fatigue group 1, see Fig. 17. Due to the larger fatigue load range in fatigue group 1, for each type of test specimens, under loading state, comparatively larger maximum crack widths at the two lateral surfaces are presented in test specimens of fatigue group 1, see Tables 4-6. Slightly larger maximum increment of steel strain is presented in test specimens of fatigue group 1, see Figs. 7, 10 and 13.

So, it can be concluded that, for uncoated specimens, E0.2 specimens (i.e., 200-μm epoxy coating) and E0.6 specimens (i.e., 600-μm epoxy coating) in three groups, when they were subjected to different fatigue loads with the same fatigue cycles, the larger fatigue load range and upper limit result in larger absolute mid-span deflection, maximum crack widths at the two lateral surfaces, maximum increment of steel strain and concrete strain of each type of test specimens. This larger fatigue load range and the load upper limit make rapid tension stiffening decay in the test specimens. Considering the adverse effect of fatigue load on test specimens with thick epoxy coating thickness, as mentioned above, for epoxy-coated specimens with thicker coating thickness, this adverse effect becomes more noticeable; on the other hand, comparatively lower fatigue load range and load upper limit may have limited effect on the service performance of epoxy-coated specimens with thicker coating thickness.

When considering test specimens in groups 2 and 3, in most cases, the increment of the load cycles do increase the absolute mid-span deflections of each type of test specimens in group 3, see Fig. 16. However, it seems that the increment of the loading cycles has limited effect on the maximum increment of steel and concrete strains as well as the maximum crack widths, see Figs. 10 and 13, Fig. 17 as well as Tables 5-6. In addition, due to the comparatively lower fatigue load range and load upper limit (about 32%-35% of the yielding load of the control RC test specimens), slight performance difference is presented between the test specimen containing coated and uncoated reinforcing bars although the maximum crack widths of the epoxy-coated test specimens become slightly larger than those of the uncoated test specimens with the increase of the fatigue cycles, see Table 6.

Although it was mentioned in the previous research work (Treece and Jirsa 1989, Cleary and Ramirez 1993, Hasan *et al.* 1996) that wider cracks were presented in the specimens containing epoxy-coated bars, these wider cracks may also be related to the corresponding load conditions, for instance, the bond failure load in Treece and Jirsa (1989) and the nearly upper fatigue load limit used in Cleary and Ramirez (1993) and Hasan *et al.* (1996). In the field surveys, actual in-service load conditions of the RC elements with epoxy-coated reinforcing bars should also be considered.

6. Summary and conclusions

In order to study how the service performance of the RC elements with epoxy-coated bars is influenced by different levels of in-service loads and the actual coating thicknesses of the epoxy-coated bars, 15 RC test specimens with uncoated and epoxy-coated reinforcements was experimentally loaded under different fatigue loads, where two fatigue loadings and two fatigue cycles were considered. Three types of reinforcing bars, i.e., uncoated bars, coated bars with nominal coating thicknesses 200 μm and 600 μm were used in the RC test specimens. Test results of fatigue loading of three fatigue groups are presented. Effects of different coating thicknesses and different fatigue loads on the service performance of RC test specimens are discussed. The following conclusions are obtained:

1) For the test specimens subjected to fatigue load with larger load range and load upper limit, where the fatigue load upper limit is about 41%-45% of the yielding load of the control RC test specimens, larger mid-span deflection-load ratio, larger maximum increment of steel strain (rapid tension stiffening decay) and maximum increment of concrete strain in extreme edge of compressive zone and wider crack width are presented. When the load range and fatigue load upper limit are comparatively lower, where fatigue load upper limit is about 32%-35% of the yielding load of the control RC test specimens, the above mentioned performance of the test specimen with coated and uncoated reinforcing bars differs slightly.

2) For the test specimens subjected to the comparatively lower fatigue loads, the increment of the crack width in the epoxy-coated RC specimens with thinner coating is negligible. With the increments of the coating thickness and the in-service loading level, i.e., fatigue load range, load upper limit and fatigue cycles, the adverse factor resulting from the thicker coating thickness becomes noticeable.

3) For epoxy-coated test specimens without any initial cracks before loading, when they are subjected to the same fatigue load (same fatigue load range and load upper limit as well as loading cycles), test specimens with thicker coating thickness have wider maximum crack widths than test specimens with thinner coating.

4) For test specimens with an initial crack, when they are subjected to larger fatigue loading with larger range and load upper limit, similar effects of the initial crack on the increment of the maximum crack width of the test specimen are presented with the increment of the loading cycles; when they are subjected to fatigue load with lower range and lower load upper limit, the maximum crack width in the surface with initial crack is increased by the initial crack at the early stage of the loading test; with the increment of the loading cycles, the influence of the initial crack on the increment of the maximum crack width decreases.

For most RC specimens with epoxy-coated reinforcing bars under their in-service environments, they are subjected to different types of service loads. Most of those service loads are repeated. The service performance of test specimens with epoxy-coated reinforcing bars is greatly influenced by the in-service loading level, i.e., fatigue load range, load upper limit and fatigue loading cycles. Under the comparatively lower service load, the wider cracks of the RC specimens resulting from the use of the comparatively thicker epoxy-coated reinforcing bars may be voided. This conclusion can help to explain the better corrosion behavior of the epoxy-coated reinforcing bars obtained from field surveys, where the real in-service loads are comparatively lower than the maximum in-service loads of the RC elements.

It should be pointed out, that three-point loading arrangement was adopted in the present paper, which is inferior to four-point bending with a constant moment zone for observations of crack control. In addition, distribution bars are likely to have influence on crack formation, and hence crack spacing and crack widths. Influence of these factors on the service performance of RC test specimens in the present experiment is not discussed.

Acknowledgments

The authors gratefully acknowledge the support provided by the National Natural Science Foundation of China (No. 51178266).

References

Abrishami, H.H., Cook, W.D. and Mitchell, D. (1995), "Influence of epoxy-coated reinforcement on response of normal and high-strength concrete beams", *ACI Struct. J.*, **92**(2), 157-166.

Cairns, J. (1994), "Performance of epoxy-coated reinforcement at the serviceability limit state", *Proceedings of the Institution of Civil Engineering Structures and Buildings*, **104**(1), 61-73.

Cairns, J. and Abdullah, R. (1994), "Fundamental tests on the effect of an epoxy coating on bond strength", *ACI Mater. J.*, **91**(4), 331-338.

Cairns, J. and Abdullah, R.B. (1995), "Influence of rib geometry on strength of epoxy-coated reinforcement", *ACI Struct. J.*, **92**(1), 23-27.

Castro, P.F. (1996), "Influence of coatings on bar-concrete bond", *J. Mater. Civ. Eng.*, **8**(4), 212-214.

Cleary, D.B. and Ramirez, J.A. (1991), "Bond strength of epoxy-coated reinforcement", *ACI Mater. J.*, **88**(2), 146-149.

Cleary, D.B. and Ramirez, J.A. (1993), "Epoxy-coated reinforcement under repeated loading", *ACI Struct. J.*, **90**(4), 451-458.

Cusson, D., Qian, S., Chagnon, N. and Baldock, B. (2008), "Corrosion-inhibiting systems for durable concrete bridges. I: five-year field performance evaluation", *J. Mater. Civ. Eng.*, **20**(1), 20-28.

De Anda, L., Courtier, C. and Moehle, J.P. (2006), "Bond strength of prefabricated epoxy-coated reinforcement", *ACI Struct. J.*, **103**(2), 226-234.

Erdoğdu, Ş., Bremner, T.W. and Kondratova, I.L. (2001), "Accelerated testing of plain and epoxy-coated reinforcement in simulated seawater and chloride solutions", *Cement Concrete Res.*, **31**(6), 861-867.

Fanous, F. and Wu, H. (2005), "Performance of coated reinforcing bars in cracked bridge decks", *J. Bridge Eng.*, **10**(3), 255-261.

Fei, J. and Darwin, D. (1999), "Fatigue of high relative rib area reinforcing bars", Ph.D. Diessertation, University of Kansas Center for Research, Kansas, U.S.A.

Fib Task Group Bond Models (2000), *State-of-Art Report on Bond of Reinforcement in Concrete*, 232-235.

GB50010-2010 (2010), *Code for Design of Concrete Structures*, National Standards of People's Republic of China, Beijing, China.

Hamad, B.S. (1995), "Comparative bond strength of coated and uncoated bars with different rib geometries", *ACI Mater. J.*, **92**(6), 579-590.

Hamad, B.S., Jirsa, J.O. and D'Abreu de Paulo, N.I. (1993), "Anchorage strength of epoxy-coated hooked bars", *ACI Struct. J.*, **90**(2), 210-217.

Hasan, H.O., Cleary, D.B. and Ramirez, J.A. (1996), "Performance of concrete bridge decks and slabs reinforced with epoxy-coated steel under repeated loading", *ACI Struct. J.*, **93**(4), 397-403.

Idun, E.K. and Darwin, D. (1999), "Bond of epoxy-coated reinforcement: Coefficient of friction and rib face angle", *ACI Struct. J.*, **96**(4), 609-615.

JG3042-1997 (1997), *Epoxy Resin Coated Steel Bars*, Construction Industry Standard of the People's Republic of China, Beijing, China.

Johnston, D.W. and Zia, P. (1984), "Bond fatigue of epoxy coated reinforcing bars", *Mater. Struct.*, **17**(1), 30-34.

Kayyali, O.A. and Yeomans, S.R. (1995), "Bond and slip of coated reinforcement in concrete", *Construct. Build. Mater.*, **9**(4), 219-226.

Lau, K., Sagüés, A.A. and Powers, R.G. (2010), "Corrosion of epoxy-coated rebar in marine bridges-part 2: Corrosion in cracked concrete", *Corros.*, **66**(6), 0650021-06500216.

Lawler, J.S., Krauss, P.D., Kurth, J. and McDonald, D. (2011), "Condition survey of older west Virginia bridge decks constructed with epoxy-coated reinforcing bars", *Transp. Res. Rec.: J. Transp. Res. Board.*, **2220**, 57-65.

Manning, D.G. (1996), "Corrosion performance of epoxy-coated reinforcing steel: North American experience", *Constr. Build. Mater.*, **10**(5), 349-365.

Montes, P., Bremner, T.W. and Kondratova, I. (2004), "Eighteen-year performance of epoxy-coated rebar in a tunnel structure subjected to a very aggressive chloride-contaminated environment", *Corros.*, **60**(10), 974-981.

Oh, B.H. and Kim, S.H. (2007), "Realistic models for local bond stress-slip of reinforced concrete under repeated loading", *J. Struct. Eng.*, **133**(2), 216-224.

Rehm, G. and Eligehausen, R. (1979), "Bond of ribbed bars under high cycle repeated loads", *ACI J.*, **76**(2), 297-309.

Sagüés, A.A., Lau, K., Powers, R.G. and Kessler, R.J. (2010), "Corrosion of epoxy-coated rebar in marine bridges-part 1: A 30-year perspective", *Corros.*, **66**(6), 0650011-06500113.

Selvaraj, R., Selvaraj, M. and Iyer, S.V.K. (2009), "Studies on the evaluation of the performance of organic coatings used for the prevention of corrosion of steel rebars in concrete structures", *Prog. Org. Coat.*, **64**(4), 454-459.

Smith, J.L. and Virmani, Y.P. (1996), "Performance of epoxy-coated rebars in bridge decks", *Public Roads*, **60**(2), 6-12.

Sohanghpurwala, A.A. (2005), "Condition and performance of epoxy-coated rebars in bridge decks of the state of Pennsylvania and New York", *Proceedings of the Structures Congress and the Forensic Engineering Symposium, American Society of Civil Engineers*, New York, U.S.A., April.

Treece, R.A. and Jirsa, J.O. (1989), "Bond strength of epoxy-coated reinforcing bars", *ACI Mater. J.*, **86**(2), 167-174.

Venkatesan, P., Palaniswamy, N. and Rajagopal, K. (2006), "Corrosion performance of coated reinforcing bars embedded in concrete and exposed to natural marine environment", *Prog. Org. Coat.*, **56**(1), 8-12.

Walraven, J.C. (2008), *Eurocode 2, Design of Concrete Structures, EN1992-1-1*, Brussels, Belgium.

Weyers, R.E., Pyc, W., Zemajtis, J., Liu, Y., Mokarem, D. and Sprinkel, M.M. (1997), "Field investigation of corrosion-protection performance of bridge decks constructed with epoxy-coated reinforcing steel in Virginia", *Transp. Res. Rec.: J. Transp. Res. Board*, **1597**, 82-90.

Yeih, W., Chang, J.J. and Tsai, C.L. (2004), "Enhancement of the bond strength of epoxy coated steel by the addition of fly ash", *Cement Concrete Compos.*, **26**(4), 315-321.

CC